ACS Combinatorial Science

Research Article

pubs.acs.org/acscombsci

Investigations on Bactericidal Properties of Molybdenum−Tungsten Oxides Combinatorial Thin Film Material Libraries

Cezarina Cela Mardare[†] and Achim Walter Hassel*[,†,‡]

[†]Christian Doppler Laboratory for Combinatorial Oxide Chemistry at the [‡]Institute for Chemical Technology of Inorganic Materials, Johannes Kepler University Linz, Altenberger Strasse 69, 4040 Linz, Austria

ABSTRACT: A combinatorial thin film material library from the molybdenum−tungsten refractory metals oxides system was prepared by thermal coevaporation, and its structural and morphological properties were investigated after a multiple step heat treatment. A mixture of crystalline and amorphous oxides and suboxides was obtained, as well as surface structuring caused by the enrichment of molybdenum oxides in large grains. It was found that the oxide phases and the surface morphology change as a function of the compositional gradient. Tests of the library antimicrobial activity against *E. coli* were performed and the antimicrobial activity was proven in some defined compositional ranges. A mechanism for explaining the observed activity is proposed, involving a collective contribution from (i) increased local acidity due to the enrichment in large grains of molybdenum oxides with different stoichiometry and (ii) the release of free radicals from the $W_{18}O_{49}$ phase under visible light.

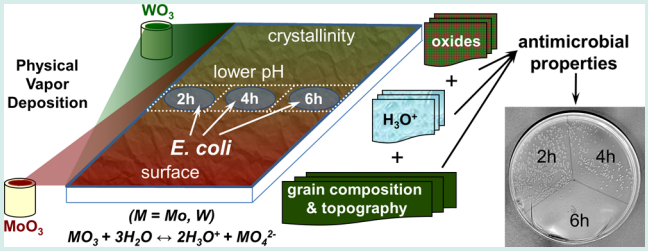

KEYWORDS: *combinatorial thin film material library, molybdenum−tungsten oxides, surface structuring, antibacterial properties*

1. INTRODUCTION

Health care associated infections (nosocomial infections) are nowadays one of the major routes through which patients requiring hospitalization may contract diseases leading to complications and, in some cases, even to death.[1] The large use of currently available antibiotics and the lack of new ones coming on the market, together with the development of antibiotic resistant bacteria like Methicillin-resistant *Staphylococcus aureus* (MRSA) or vancomycin-resistant enterococci (VRE) expose patients to high risks. Recent studies have shown that inanimate surfaces in hospitals (instruments and sanitary installations, doorknobs, switches, etc.) are a reservoir of microorganisms.[2] The biggest issue is that the microorganisms' transmission to the patients in many cases cannot be prevented just by the hand hygiene of the healthcare workers or by disinfection, especially in the case of some special medical devices. Therefore, the development of bactericidal materials is highly needed, in order to prevent the proliferation of microorganisms and their transfer to patients.[3] Currently, there are two main approaches to decrease the contamination of inanimate surfaces, by either preventing their adhesion onto the surface and/or by having a biocidal effect. Antiadhesive coatings such as diamondlike-carbon, self-cleaning surfaces, or poly(ethylene glycol) prevent microorganism adhesion, but they have the major drawback in moving them around instead of eliminating them. Coatings with biocidal effect (Ag- and Cu-containing coatings, photocatalysts, polycationic surfaces) are effective in killing them but still show some issues like cytotoxicity or development of resistance to infectious agents.[4] Consequently, there is a great need for the development of new coatings, which are both safe and able to decrease and prevent the contamination, transmission, and growth of microorganisms onto inanimate surfaces close to patients.

It was recently reported that molybdenum oxides and suboxides powders embedded in polyurethane tubes,[5] coated onto lead wires,[6] and electrodeposited into TiO_2 nanotubes[7] show very promising properties as antibacterial materials against many nosocomial agents such as Gram-negative and spore-forming microorganisms and against two staphylococci. The authors explained the bactericidal effect of molybdenum oxide by the formation of acidic surfaces in the presence of humidity and at pH < 6 via the following reaction:[8]

$$MoO_3 + 3H_2O \leftrightarrow MoO_4^{2-} + 2H_3O^+$$

The aforementioned reaction refers not only to molybdenum oxide, but to transition metal oxides in general. Thus, it has been suggested to function also for tungsten oxide,[9] with the formation of WO_4^- and/or WO_4^{2-} at similar pH values as in the case of molybdenum oxide.[10]

Even though there are many applications for which powders or nanostructures can be used for preventing the development of microorganisms onto inanimate surfaces, for antibacterial coatings thin films can be used as functional surfaces. The one-by-one sample preparation approach requires a lot of time and energy and some enhanced properties can be easily missed simply because a specific composition has never been

Received: April 2, 2014
Revised: October 12, 2014
Published: October 20, 2014

   dx.doi.org/10.1021/co5000536 | *ACS Comb. Sci.* 2014, 16, 631−639

addressed. On the other hand, thin film synthesis involving spatial variation of composition can be used for producing combinatorial libraries or compositional spreads.[11] In the last years, the combinatorial solid-state chemistry led to the discovery of new materials with outstanding properties.[12] As an example, this method has already been applied successfully in the thin film area for the Co-doped TiO_2 thin films, revealing that TiO_2 becomes photocatalytically active under visible light only for a restricted Co content, between 5.4 and 9 at %.[13] It was also recently used for finding mixed amorphous Hf–Ta oxides with applications for high dielectric constant materials,[14] for enhanced photoelectric effects in iron oxide–tungsten oxide thin film libraries,[15] or for catalysts for oxygen reduction reaction.[16] Concerning mixed Mo–W oxide thin films, there are many reports involving discrete compositions and deposition techniques such as sol–gel,[17] cathodic electrodeposition,[18] chemical vapor deposition (CVD),[19] thermal evaporation,[20] RF sputtering,[21] spray pyrolysis,[22] or liquid phase deposition,[23] with the main research focus on the investigation of optical, electrochromic, and gas sensing properties. To the best of the authors' knowledge, no combinatorial approach was applied to this oxides system, either for a structural and morphological study, or as antimicrobial coatings, even though some promising results on mixed molybdenum–tungsten oxides with discrete compositions were already reported in the literature.

Herein, the authors report on the preparation and characterization of a molybdenum and tungsten oxides combinatorial thin films material library deposited by thermal coevaporation, as well as a screening of antimicrobial properties as a function of compositional change. The main advantage of this method as compared with the one-by-one approach is that the samples with a compositional spread have the same history (identical deposition and heat treatment conditions), therefore the results obtained are directly comparable and often more consistent.

2. EXPERIMENTAL DETAILS

2.1. Combinatorial Thin Film Material Libraries. Molybdenum oxide (HC Starck, Germany) and tungsten oxide (Wolfram Bergbau und Hütten AG, Austria) powders were used as precursors for the thin film material library deposition. Microscopy glass slides (76 mm × 24 mm) were cut in 18 chips, and they were cleaned in an ultrasonic bath in acetone, followed by isopropanol. Afterward, they were rinsed with water, dried under nitrogen flow, and subsequently placed inside the vacuum chamber. The material library deposition was performed using an in-house developed thermal coevaporation system.[15] The system was pumped until a base pressure of approximately 5×10^{-6} hPa was reached to ensure low levels of impurities in the films. The MoO_3 and WO_3 powders were placed in separated alumina crucibles positioned at a distance of 120 mm from the substrate directly below each of the two short sides of the substrates. This geometry leads to the formation of a compositional gradient along the substrate due to vapor phase mixing of both oxides. The evaporation sources were powered by individual DC sources able to provide up to 3.5 kW each. The minimum power needed for evaporation was 150 W for MoO_3 and 400 W for WO_3. By adjusting the power on each source, the evaporation rates of each material can be tuned and therefore the compositional spread along the substrate can be adjusted as desired. By modifying the distance between either of the two sources and the substrate, the compositional gradient can be compressed along the substrate (e.g., steep concentration change), thus conferring the possibility of properties screening over a wide compositional range. Also, the compositional gradient can be stretched (e.g., just a few percentage spread along the entire substrate length), consequently providing the possibility to address with an increased compositional resolution very specific compositions. In the current work, the evaporation rates (approximately 1 nm s^{-1} for both materials) were actively tuned during the deposition process via a self-developed proportional–integral–derivative (PID) controller in order to achieve a large compositional spread along the substrate. This was desired because the aim is to investigate a broad compositional range, for the initial screening of the bactericidal properties of a MoO_3–WO_3 mixed system. The as-deposited thin films were heat treated in ambient air with 1 K min^{-1} heating and cooling rates in a multiple step process, as follows: heating to 300 °C, sinking time 2 h, cooling to 20 °C, heating to 400 °C, sinking time 4 h, cooling to 20 °C. Figure 1a shows the photograph of such material library. Each of the 18 chips had approximately 12 mm × 8 mm, and they were arranged in three rows with six chips on each row. The arrow in the upper part of the figure indicates the side along which the composition spread was deposited, whereas the arrow across the sample indicates a constant composition.

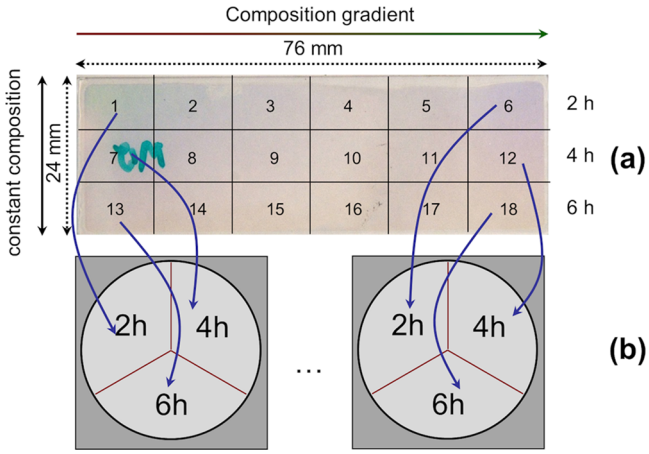

Figure 1. (a) Photograph of a Mo–W oxides thin film material library deposited on glass indicating the chips (1–18), the direction of the Mo gradient, and the positions wherefrom the bacterial culture was harvested after defined times. (b) Schematic drawing of the agar plates.

The surface morphology before and after the heat treatment, as well as the compositional spread along and across the substrate, were measured using a Zeiss 1540-XB field emission scanning electron microscope (FE-SEM) with a build-in energy dispersive X-ray spectrometer (EDX) from INCA X-Sight Oxford Instruments. The measurement was performed using a 20 kV accelerating voltage, and the results were analyzed using the INCA-software. The surface topography was visualized using an atomic force microscope (AFM) Nanosurf Easyscan 2. The crystallinity of the thin film material libraries was investigated using a Philips X'Pert Pro X-ray Diffraction (XRD) system using Cu Kα radiation and working in either grazing incidence ($\omega = 0.51°$) or Bragg–Brentano geometry. The spot size was adjusted in such way that only one chip at a time was measured; therefore, a scanning of the crystalline phases along the compositional gradient was obtained. The phase identification was done with the X'Pert HighScore Plus software using the PDF 2 database.

2.2. Antibacterial Testing. Bacterial cultures were prepared from 10 μL frozen stock of *Escherichia coli* (*E. coli*) strain BL21DE3 (kanamycin resistant) kept in glycerol at −18 °C and inoculated in 1 mL of Lysogeny Broth (LB) medium. The medium was incubated for 18 h at 37 °C under continuous motion in a rotary shaker. The working culture was prepared by diluting 1 μL of the cells culture in 1 mL of LB medium. An optical density $OD_{580\ nm} = 0.1$ of the culture corresponding to ~10^6 CFU mL^{-1} was measured using a Kontron Uvikon 800 system. The LB medium was prepared by mixing yeast extract (USB Corporation), NaCl 99.97% purity (Merck), and casein (USB Corporation) in distilled water. Subsequently, the solution was sterilized and after cooling down to approximately 50 °C, kanamycin (stock solution 30 mg mL^{-1}) was added. Agar plates were used as culture medium, and the details of this procedure are summarized in Table 1.

dx.doi.org/10.1021/co5000536 | ACS Comb. Sci. 2014, 16, 631–639

Table 1. Chemicals Used for the Preparation of LB Medium and the Agar Plates, Together with the Sterilization Conditions

	yeast extract/g	NaCl/g	casein/g	agar/g	sterilization	kanamycin/mL
LB medium (1 L)	5	10	10	0	autoclaving at 125 °C for 10 min	1
agar plates (1 L)				20		

On each glass chip coated with the molybdenum−tungsten oxides thin film library, a droplet of 40 μL from the working culture was applied. Here it is worth mentioning that 18 (3 rows with 6 chips per row) was the maximum useful number of chips which could be obtained from a library. This conclusion was reached considering two aspects: (1) the minimum area (approximately 100 mm^2) required for the 40 μL of working culture to cover fully the surface of one chip but not to flow out of it and (2) for the same composition spread, three chips were needed for three different testing times (2, 4, and 6 h). After one defined time, 20 μL of liquid was harvested from the surface of each chip (along one row in Figure 1a for a defined time interval) and diluted in 1 mL of sterile phosphate buffered solution (PBS) having a pH of 7.4. A volume of 10 μL from the PBS with bacteria solution was evenly spread in the designated area onto the agar plates prepared as indicated in Table 1. This procedure was applied in order to assess the "volume activity" as a function of the compositional gradient, namely the influence of the coating on the bacterial growth for bacteria floating in fluid in the vicinity of the coating's surface. Each chip with the remaining 20 μL of working culture was rinsed thoroughly in sterile PBS for removing the bacteria unattached to the surface. Subsequently, each chip was placed in an Eppendorf vial in 1 mL of PBS and placed in a vortex at 2000 rpm for 2 min in order to detach the bacteria fixed on the coating's surface. In the following step, 10 μL from the PBS with bacteria solution was harvested and spread onto the agar plate. The purpose of this procedure was to assess the "surface activity" of the Mo−W oxides, namely the influence of both compositional gradient and surface structuring on the bacterial growth.[24] The agar plates were incubated for 12 h at 37 °C. Consequently, one individual chip was used for two experiments (both volume and surface activity), three chips with identical compositions (along one column in Figure 1a) show the activity as a function of time, whereas the six chips along one row in Figure 1a indicate the activity as a function of the compositional gradient. Figure 1b shows a schematic drawing of the agar plates. Each plate corresponds to one concentration spread (three chips across the library), and it was divided into three parts each corresponding to a defined time interval (2, 4, and 6 h). There were 15 plates in total, 6 used for testing the volume activity, 6 for testing the surface activity, and 3 more for the positive and negative control.

3. RESULTS AND DISCUSSION

3.1. Characterization of Combinatorial Mo−W Oxide Thin Film Libraries. The as-deposited Mo−W oxide thin film material libraries had a thickness in the range of 450−500 nm measured in situ by quartz crystal microbalances (QCMs). Figure 2 shows the compositional spread obtained along the library as measured by EDX. The left and right *y*-axis represent the Mo and respectively W concentrations in atom percent, and the *x*-axis indicates the sample nomenclature.

The plot shows four concentration values for each chip. They represent the concentrations (Mo and W) at two extremities of each chip in the direction of concentration change, thus offering information on the exact local composition spread along each chip. In turn, this will define the local compositional resolution of the study. The EDX results are given with respect to the metal concentrations and do not include oxygen. This method of quantification (only considering the metals) was chosen due to the fact that both the films and the glass substrates contain oxygen. Consequently, a quantitative oxygen analysis in the EDX would not be meaningful for coatings having a few hundred nanometer thickness, since the measured oxygen

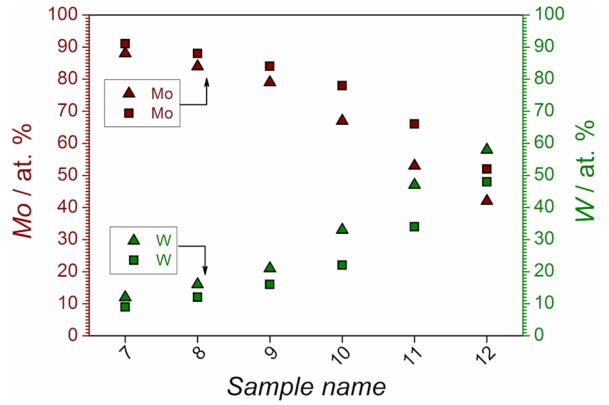

Figure 2. Compositional spread (relative to the metal bases) of the Mo−W oxide thin film library along the central row (samples 7−12) indicating the Mo and W concentrations (in at %) near the edges of each chip. A pair of red and green squares represents the concentrations of Mo and W on one edge of a chip, whereas the pair of red and green triangles represents the Mo and W concentrations at the opposite edge on the same chip.

content will include both film and substrate. Therefore, the concentrations should be read accordingly in the entire data analysis and discussion. The EDX characterization (Figure 2) showed a compositional gradient along the library ranging from approximately 91 at % Mo in one side (and 9 at % W, respectively) to 44 at % Mo (56 at % W, respectively). On each chip five different points were measured (on all four edges and in the center) in order to quantify an exact local compositional spread. The nonlinearity in the concentration was expected, and it is caused by the particular geometry of the used coevaporation system (with relatively small deposition distances)[25] and to the cosine law of evaporation.[26] Consequently, comparing the local compositional spreads along each chip, it can be seen that the local concentration change was not a constant along the library. This ranged from approximately 2 at % in the Mo-rich side up to 11 at % in the W-rich side. Across the library there was found no concentration gradient.

The XRD investigations on the as-deposited films revealed that they are amorphous independently on the composition. This was expected, since in thermal evaporation processes the energy of the evaporated species is low (0.1−0.2 eV). Therefore, the atoms/molecules arriving at the substrate do not have enough energy for surface diffusion activation, which is a necessary condition for crystallization on a (cold) substrate.[27] Figure 3a shows as an example the XRD pattern for an as-deposited sample with the composition at the center of 70 at % Mo. After the first heat treatment at 300 °C, the films show the beginning of crystallization with only one broad peak being present at $2\theta = 22.8°$ (Figure 3b). This peak might be related to the crystallization of molybdenum oxide, since the temperature threshold for the beginning of crystallization in amorphous molybdenum oxide is lower than the one for tungsten oxide.[28] Nevertheless, solely from one peak it is difficult to state with certainty to which phase/oxide it belongs.

dx.doi.org/10.1021/co5000536 | ACS Comb. Sci. 2014, 16, 631−639

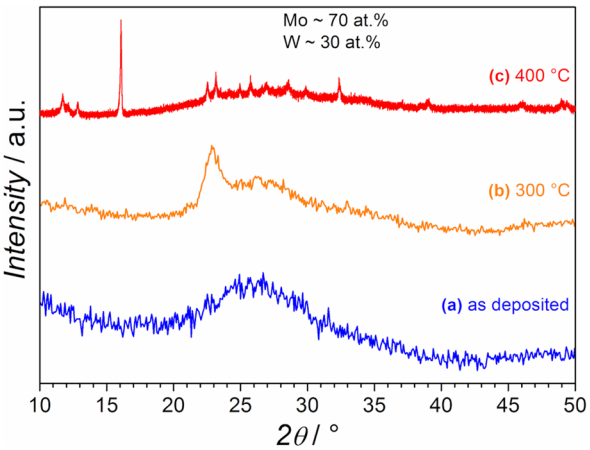

Figure 3. Comparison of the XRD patterns for a sample with approximately 70 at % Mo and 30 at % W in the center: as deposited (a), after 2 h at 300 °C in ambient air (b), and after 4 h at 400 °C in ambient air (c).

After the second heat treatment temperature at 400 °C, the films show higher crystallinity. Figure 3c shows the XRD pattern for a sample with the same composition as in Figure 3a and b, but after the heat treatment at 400 °C.

As already indicated by the pattern in Figure 3c, the Mo−W oxide thin film library shows a higher degree of crystallinity after the second heat treatment. Figure 4 presents the change of

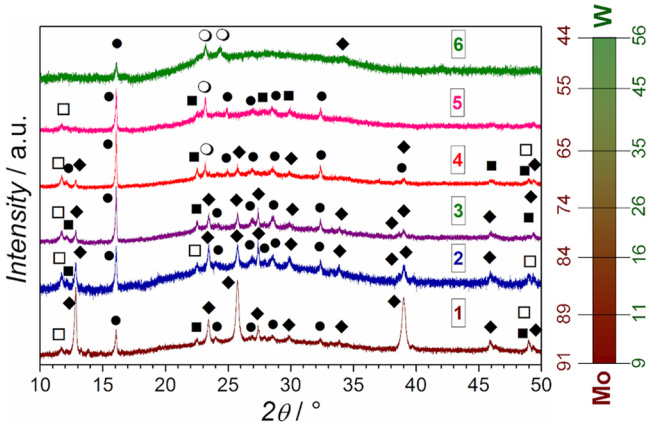

Figure 4. XRD patterns along the Mo−W oxide library after the heat treatment at 400 °C showing the changes of oxide phases as a function of compositional change. The identification of present phases is ◆ α-MoO_3, □ Mo_9O_{26}, ■ $Mo_{17}O_{47}$, ● $W_{18}O_{49}$, ○ m-WO_3.

the crystalline phases as a function of the compositional spread along the library. The insets with numbers from 1 to 6 represent the sample and the corresponding XRD pattern. The color bar on the right side of the graph indicates the compositional spread along each measured sample.

The phases found in the Mo rich side are α-MoO_3, the Magnéli phase Mo_9O_{26},[29] $Mo_{17}O_{47}$, and the $W_{18}O_{49}$ stoichiometric oxide. Among the many W-oxide possible phases, the $W_{18}O_{49}$ seems to show the best match, also being in agreement with the data reported by Taurino et al. for films with similar composition and heat treatment temperatures.[17] The $W_{18}O_{49}$ phase together with α-MoO_3 and the monoclinic WO_3 could be found for samples 4−6 with the W content >30 at %. No mixed $(Mo_{1-x}W_x)O_3$ phases could be clearly matched with any of the patterns. It is presumed that the lack of mixed phases is related with the multiple step heat treatment performed. The MoO_3 crystallization temperature is lower than the one from WO_3, therefore after the first heat treatment mainly the molybdenum oxides start to crystallize, while tungsten oxide is still amorphous. Only during the second heat treatment the tungsten oxide crystallization occurs, but since the molybdenum oxides are already crystalline (or partially crystalline), the solid state diffusion is probably low, preserving phase separation between the molybdenum and tungsten oxides. Since the atomic radii of Mo and W are very similar, it is not supposed that pure phases segregate, but rather W being solute in molybdenum oxides (and Mo in tungsten oxides) in sufficiently low amounts not to lead to the formation of $(Mo_{1-x}W_x)O_3$ mixed oxide phases. Another possibility is that the content of these mixed oxide phases is low enough not to give a significant signal in the XRD patterns. With increasing the W concentration, it also can be observed that the peaks intensities decrease and the background signal has a more pronounced curvature. A strong contribution from the glass substrate to this amorphous phase is not likely to occur since the thickness of the thin film does not differ greatly along the sample and in the Mo-rich region the broad background signal is considerably lower. Thus, this is an indication that the tungsten oxide is not fully crystalline, but there is an amorphous part present as well. This aspect has already been reported in the literature for thin films with the Mo:W ratio of 90:10 and 80:20 (at % : at %) deposited by liquid phase deposition and postdeposition annealed at 200 and 500 °C.[23] Similar results were found for Mo−W oxide thin films deposited by CVD at 200 °C, followed by postannealing at 400 °C[30] and 500 °C.[19]

The phase separation is supported by the SEM imaging/EDX analysis performed on the surface of the samples after the heat treatments (Figure 5). The images shown in Figure 5 were acquired in three regions along each chip (edges - (a), (b) and center - (c)). In general, different surface microstructures can be observed. For the sample 1a, with the highest Mo content, a two layer structure is visible. The outermost layer shows some porosity and the presence of elongated grains with a length up to a few μm, whereas the layer underneath seems to be composed only of much smaller needle-like grain structure, also not fully compacted. With increasing the W content, it can be clearly seen that the previously underneath layer becomes more and more visible onto the surface, and simultaneously some islands of crystals with different morphology develop (e.g., sample 3c). These islands of crystals which have a very structured surface are further converted to large domains with some small outgrown grains with a length in the range of few hundred nm (e.g., sample 5a). At even higher W content, the surface shows another type of structuring, with clearly separated grains with a length in the μm range, surrounded by a layer that appears much smoother, but porous (6b). This porosity has already been reported in the literature and it is related to the high Mo mobility which diffuses toward the surface and leads to the segregation of molybdenum oxide rich phases, consequently resulting in the formation of a tungsten oxide rich porous layer underneath.[31]

The EDX measurements performed in different areas (Table 2) confirm the hypothesis that the molybdenum oxide crystallizes first, leading to a phase separation with molybdenum oxide rich regions on top of tungsten oxide rich regions. Big difference in the compositions in neighboring areas can be observed. For example, on the sample 1a, the

dx.doi.org/10.1021/co5000536 | ACS Comb. Sci. 2014, 16, 631−639

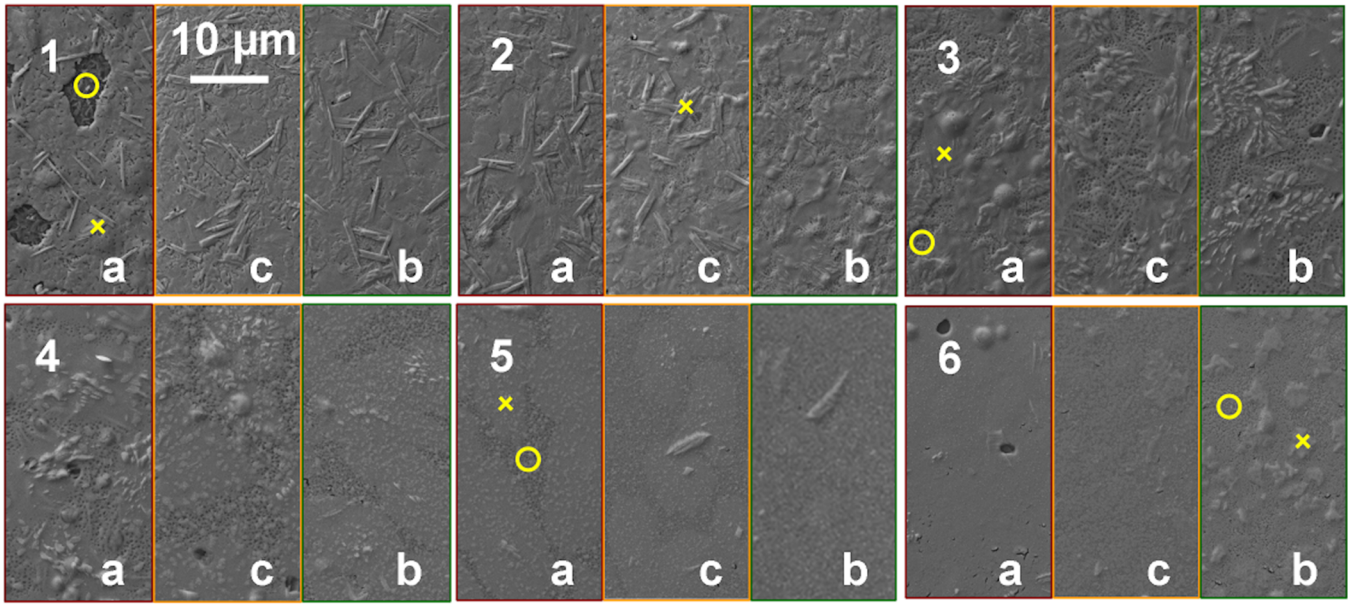

Figure 5. SEM images of the Mo–W oxide thin film library after the multiple step heat treatment showing the change of the surface microstructure as a function of compositional change. Along each sample (numbered from 1 to 6 in the upper left side) three different regions are shown: (a) and (b) were acquired near opposite edges in the direction of the compositional gradient, and (c) in the center. The circle and cross indicate the selected areas where EDX measurements were performed.

Table 2. Composition in Different Areas along the Mo–W Oxides Thin Film Library Comparing the Overall Composition and the Ones in Different Adjacent Regions, Which Show Different Surface Morphologies

Sample	1a		2c		3a		5a		6b	
At %	Mo	W	Mo	W	Mo	W	Mo	W	Mo	W
Overall	91	9	85	15	83	17	63	37	57	43
Circle	68	32	-	-	79	21	57	43	43	57
Cross	90	10	89	11	82	18	67	33	67	33

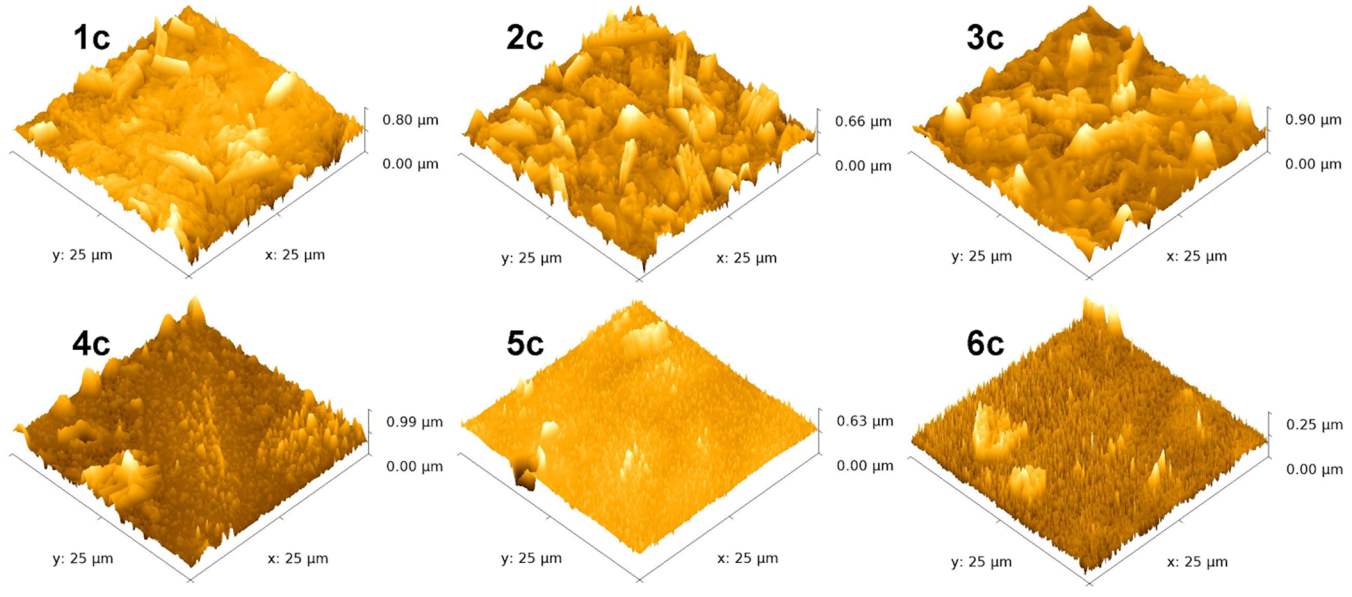

Figure 6. AFM images acquired in the center of each sample along the Mo–W oxide thin film library after the multiple step heat treatment.

composition of the layer closer to the substrate (circle) has approximately 68 at % Mo, as compared to the composition of the outer layer (91 at % Mo). For this sample, there is not a big difference between the overall composition and the composition of a single, elongated grain (cross), which show approximately the same Mo content. This might be attributed to several factors such as small film thickness (hundreds of nanometers), large Mo content, and the integration of the EDX signal from both layers during the measurement, which leads to the impossibility of separating the signals from outer and inner

dx.doi.org/10.1021/co5000536 | ACS Comb. Sci. 2014, 16, 631–639

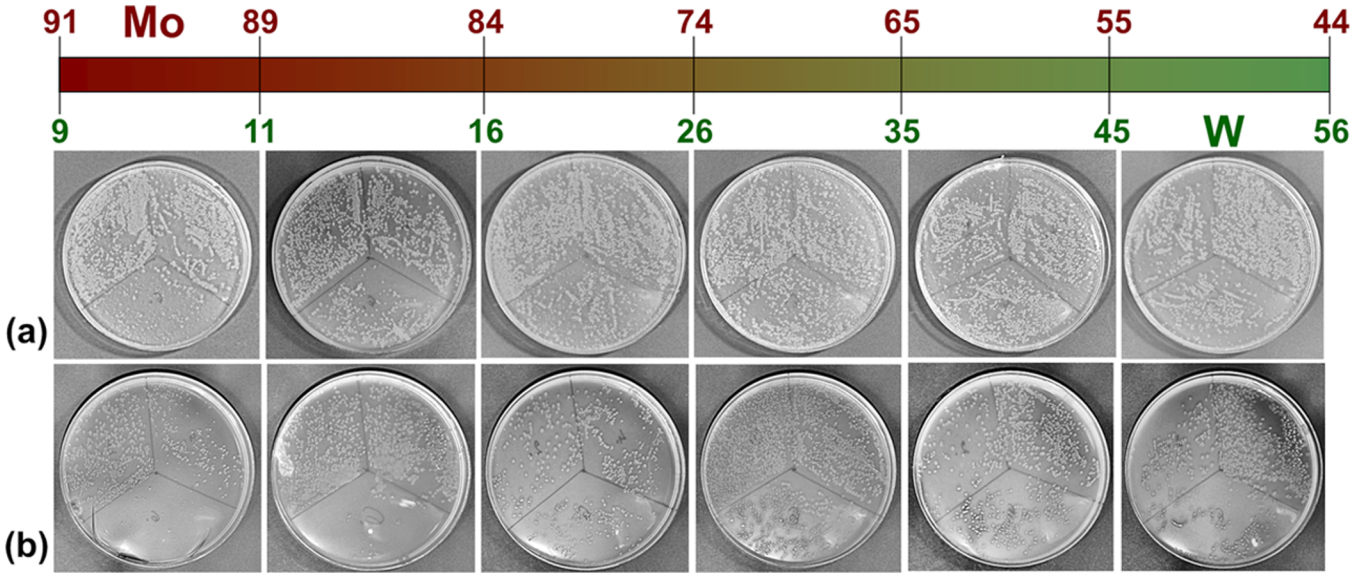

Figure 7. Agar Petri dishes showing the *E. coli* colonies grown on the Mo−W oxide thin film material libraries as a function of compositional change and of harvesting procedure: (a) from the volume and (b) from the surface.

layers in the region where the layer underneath it is not exposed. With increasing the W content, the regions with different morphologies seen in the SEM images also show large compositional variations (samples 5 and 6). For sample 6b for example, the overall composition indicates approximately 57 at % Mo, with the outgrown grains (cross) having approximately 67 at % Mo, whereas the neighboring region (circle) shows only 43 at % Mo. Also these concentrations, especially the ones from the outgrown grains, have to be understood solely as an indication of a strong enrichment of an element in the referred grains, rather than a precise value. This is due to the fact that the EDX signal comes from the entire film thickness in the measured spot, thus including a possibly tungsten oxide rich layer underneath the outgrown grain.

For a better understanding of the surface morphology after the multiple step heat treatments, the samples were investigated using AFM imaging (Figure 6). As already indicated by the SEM images, the surface morphology varies with the change in composition. In general, the molybdenum oxides rich outgrown grains protrude from the surface and reach heights up to approximately 900 nm (samples 1−4). Taking into consideration that the thin film material library thickness is in the range of 450−500 nm, it can be concluded that the underlying tungsten oxide rich layer has a smaller thickness as the overall estimated thickness of the thin film and/or a high porosity. The structuring of the surface is, as expected, more pronounced for high-Mo concentrations and becomes more uniform as the W-content increases (samples 5 and 6). This fact is probably due to the availability of molybdenum oxide, which crystallizes before the tungsten oxide. Consequently, in the regions with high Mo content, there are more molybdenum oxide rich grains. This fact is also confirmed by the SEM/EDX investigations. For example, for the highest Mo concentration the molybdenum oxide rich layer covers almost completely the tungsten oxide rich layer. As the Mo content decreases and the W content increases, there are less and not that high outgrown grains present (sample 5 and 6). The outgrown grains appear as some isolated islands, surrounded by a matrix composed of some much smaller grains which also protrude from an underlying layer.

3.2. Antibacterial Testing. The aforementioned method for the growth of the *E. coli* bacterial culture was applied for assessing the bactericidal activity of the Mo−W oxide thin film material library. By this method, not only the activity in the volume of the fluid in the surface vicinity may be investigated, but also the activity of the surface. Nevertheless, this should be seen as a comparative study to screen possible Mo−W compositions of interest and to observe if the surface structuring has an effect on the attachment of bacteria onto the surface, and not for quantitative analysis. Merely a "yes−no" testing was foreseen, in which it could be visualized if bacteria attach and proliferate onto/in the vicinity of the surface. If the material is not active, they will proliferate and be transferred to the agar plates, whereas if it is active in the duration of the experimental time, there would be no remnant bacteria which can be transferred and no colonies will grow. It is worth mentioning that also positive (Cu substrates) and negative test cultures (the working culture) were performed, in order to ensure the validity of the experiments in terms of sterile conditions and bacterial growth.

Figure 7 shows the result of this investigation as after 2, 4, and 6 h (ordered as depicted in Figure 1), with the (a) row referring to the cultures harvested from the volume, whereas the (b) row refers to the ones harvested from the surface. The color bar on top of the figure represents the concentration ranges of each set of chips with the same compositional spread. Underneath, the agar plates on which the antibacterial tests were performed with cultures harvested from the corresponding chips are shown. As a general observation, it can be seen that after 6 h incubation time and subsequent overnight growth, for some compositional ranges there were no visible colonies present for the culture harvested from the surface (Figure 7b) or much fewer than for 2 and 4 h for the ones harvested from the volume (Figure 7a). The active regions are from 91 to 74 at % Mo (9 to 26 at % W, respectively) and possibly for the samples having 55 to 44 at % Mo (45−56 at % W). When comparing the results from the volume (Figure 7a) to the ones from the surface (Figure 7b), a consistency of the activity for the same compositional range can be observed (along each column), but more colonies are present in the case of cultures

dx.doi.org/10.1021/co5000536 | ACS Comb. Sci. 2014, 16, 631−639

harvested from the volume. This is expected, since for assessing the surface activity additional steps were present. These steps included the washing of the PBS with bacterial culture for disposing of the bacteria unattached to the surface, thus decreasing the number of bacteria which were later on applied on the agar Petri dishes. Due to this consistency in terms of volume/surface activity versus composition (similar results along one column in Figure 7), but the observed nonlinearity concerning activity versus compositional change (no linear trend along the rows in Figure 7), the influence of the surface structuring might be inferred. In the regions where the activity is lower (chips 4−10−16 and 5−11−17 in Figure 1, and columns 4 and 5 in Figure 7), also the surface morphology shows a completely different microstructure in the SEM (Figure 5) and AFM (Figure 6) images as compared to the more active regions. For this compositional range (approximately 74−54 at % Mo and 26−46 at % W, respectively), the surface lacks the large, overgrown molybdenum oxide rich grains present in the regions with high Mo concentration and instead domains with smaller grains and smoother surfaces were seen. It is possible that the bacteria attachment and adhesion onto the less structured surface and/or into pores might be higher, thus leading to reduced activity of these surfaces. For the samples with the highest W content (Figure 1, chips 6−12−18, and Figure 7, last column), which also show some activity after 6 h, the larger grains rich in molybdenum oxide are again present but their coverage on the surface is not as high as in the case of regions with high Mo concentrations.

Another hypothesis for the observed nonlinear behavior might relate the changes in activity to the local changes in the pH, driven by the enrichment of neighboring regions with Mo or W.

As already mentioned, the molybdenum oxide owns its bactericidal properties to the formation of acidic surfaces in the presence of humidity. Gram-negative bacteria as *E. coli* can be killed at pH values lower than 5.5.[5] Consequently, the mechanism responsible for the observed activity of MoO_3 was assumed to be the formation of H_3O^+ ions in the vicinity of the surface leading to an increased acidity by locally lowering the pH value of the working culture.[7] A similar mechanism was proposed for WO_3.[9] In the current study, if solely this mechanism would be responsible for the observed antimicrobial activity of mixed molybdenum and tungsten oxides, there should be no variations in the activity as a function of compositional change, since they would both contribute to the increase in the acidity. Nevertheless, due to the variations in the stoichiometry and crystallinity of these oxides and to the lack of referred data concerning change of the pH caused by the presence of these mixed oxides and suboxides, this hypothesis cannot be totally disregarded.

Comparing the literature on the antibacterial properties of molybdenum oxides and suboxides to tungsten oxide, it has been reported that the latter has no antimicrobial properties,[32] or activity only under laser irradiation via a photocatalytic effect,[33] and when covered with Ag[34] or Pd nanoparticles.[35] In the present study, there was no continuous decrease of activity as a function of tungsten concentration increase, therefore it might be inferred that it also contributes to the activity. Thus, an assumption can be made that the contribution comes rather from the presence of $W_{18}O_{49}$, than from the WO_3, cumulated with the molybdenum oxide rich large grains found for some compositional ranges. $W_{18}O_{49}$ has an acidic surface due to its unique defect structure that can accommodate a large number of oxygen vacancies.[36] Promising research has been already performed for wastewater purification using nanostructured $W_{18}O_{49}$ which degrades pollutants in the presence of visible light by the formation of OH* radicals.[36,37] On the other hand, the bacterial disinfection works also in the presence of free radicals by the oxidation of the cells membrane, and the subsequent damage.[4,35] Since the present experiments were carried on under visible light, it can be presumed that the observed activity comes from a synergetic coupling of the structured surface due to the large molybdenum oxide rich grains which are responsible for the local changes in the pH, and the adjacent regions containing $W_{18}O_{49}$, which release free radicals under visible light.

4. CONCLUSIONS

In this work two new approaches were presented: (i) the preparation and characterization of Mo−W oxides combinatorial thin film libraries and (ii) the proof of principle as they can be used as antimicrobial coatings with screening compositional ranges active against *E. coli*. Combinatorial thin film coatings with compositional spreads ranging from 91 to 44 at % Mo (9 to 56 at % W, respectively) were successfully deposited by thermal coevaporation. After a multiple step heat treatment, a mixture of crystalline molybdenum and tungsten oxides and suboxides and amorphous tungsten oxide were obtained. By this type of heat treatment, also the surface structuring caused by the enrichment of molybdenum oxide in large grains was achieved. Preliminary tests of the coatings' antimicrobial activities against *E. coli* strain BL21DE3 (kanamycin resistant) were performed, by investigating the bacterial growth both onto the surface and in the volume of the working culture. In some certain compositional ranges [91−74 at % Mo (9−26 at % W, respectively)] and possibly for the samples having 55−44 at % Mo (45−56 at % W) the antimicrobial activity was proven, and some possible mechanisms were proposed. The mechanism involves a combined contribution of surface structuring and the presence of the $W_{19}O_{49}$ phase. The former is caused by the enrichment of molybdenum oxides in large, structured grains, which lower locally the pH via formation of hydroxonium ions, whereas the $W_{19}O_{49}$ phase is responsible for the formation of free radicals under visible light. Both these mechanisms were reported as factors that can damage the cell membranes leading to their death and consequently to the observed antimicrobial activity. Further investigations are planned for a more detailed screening of the exact composition(s) which are active by expanding a smaller gradient over the sample length. Also, as a proof of the working principle, a comparison of the activity under light and in the dark will be pursued, to confirm the proposed mechanism relating the presence of the $W_{18}O_{49}$ phase with the observed bactericidal effect.

AUTHOR INFORMATION

Corresponding Author

*E-mail: achimwalter.hassel@jku.at.

Notes

The authors declare no competing financial interest.

ACKNOWLEDGMENTS

The authors would like to acknowledge the help of Dr. A. I. Mardare for the thermal evaporation of the material libraries and MSc. Yulia Golitsyna and Prof. Sabine Hild from Institute of Polymer Science, JKU Linz, and MSc. Adriana Walnerova

and Prof. Dr. Norbert Müller from Institute of Organic Chemistry, JKU Linz for sharing their know-how concerning the antimicrobial testing. The financial support by the Austrian Federal Ministry of Economy, Family and Youth and the National Foundation for Research, Technology and Development is gratefully acknowledged.

REFERENCES

(1) Vincent, J.-L.; Rello, J.; Marshall, J.; Silva, E.; Anzueto, A.; Martin, C. D.; Moreno, R.; Lipman, J.; Gomersall, C.; Sakr, Y.; Reinhart, K. International Study of the Prevalence and Outcomes of Infection in Intensive Care Units. *JAMA* **2009**, *302*, 2323−2329.

(2) Dancer, S. J. How do we assess hospital cleaning? A proposal for microbiological standards for surface hygiene in hospitals. *J. Hosp. Infect.* **2004**, *56*, 10−15.

(3) Klibanov, A. M. Permanently microbicidal materials coatings. *J. Mater. Chem.* **2007**, *17*, 2479−2482.

(4) Page, K.; Wilson, M.; Parkin, I. P. Antimicrobial surfaces and their potential in reducing the role of the inanimate environment in the incidence of hospital-acquired infections. *J. Mater. Chem.* **2009**, *19*, 3819−3831.

(5) Zollfrank, C.; Gutbrod, K.; Wechsler, P.; Guggenbichler, J. P. Antimicrobial activity of transition metal acid MoO_3 prevents microbial growth on material surfaces. *Mater. Sci. Eng., C* **2012**, *32*, 47−54.

(6) Tétault, N.; Gbaguidi-Haore, H.; Bertrand, X.; Quentin, R.; van der Mee-Marquet, N. Biocidal activity of metalloacid-coated surfaces against multidrug-resistant microorganisms. *Antimicrob. Resist. Infect. Control* **2012**, *1:35*, 1−6.

(7) Lorenz, K.; Bauer, S.; Gutbrod, K.; Guggenbichler, J. P.; Schmuki, P.; Zollfrank, C. Anodic TiO_2 nanotube layers electrochemically filled with MoO_3 and their antimicrobial properties. *Biointerphases* **2011**, *6*, 16−21.

(8) Deltombe, E.; de Zoubov, N.; Pourbaix, M. Molybdenum. In *Atlas of Electrochemical Equilibria in Aqueous Solutions*, 2nd ed.; Pourbaix, M., Ed.; National Association of Corrosion Engineers: Houston, TX, USA, 1974; pp 272−279.

(9) (a) Guggenbichler, J. P.; Eberhardt, N.; Martinez, H. P.; Wildner, H. Use of an inorganic material e.g. to form a hydrogen cation for the achievement of antimicrobial effect, and as an additive material for hygienic absorbent articles or wound coverings. Patent numbers DE202006018695-U1; WO2008058707-A2; WO2008058707-A3; IN200901843-P2; EP2091333-A2; KR2009094277-A; CN101610679-A; US2010057199-A1; JP2010509385-W; RU2009117726-A; EP2428118-A2; EP2428118-A3; RU2473366-C2; CN101610679-B; JP2013209374-A; 2007. (b) Lackner, M.; Maninger, S.; Guggenbichler, J.-P. Acidic Surfaces as novel Contact Biocide. *Nachr. Chem.* **2013**, *61*, 112−115.

(10) Deltombe, E.; de Zoubov, N.; Pourbaix, M. Tungsten. In *Atlas of Electrochemical Equilibria in Aqueous Solutions*, 2nd ed.; Pourbaix, M., Ed.; National Association of Corrosion Engineers: Houston, TX, USA, 1974; pp 280−285.

(11) (a) Xiang, X.-D.; Sun, X.; Briceno, G.; Lou, Y.; Wang, K.-A.; Chang, H.; Wallace-Freedman, W. G.; Chen, S.-W.; Schultz, P. G. A Combinatorial Approach to Materials Discovery. *Science* **1995**, *268*, 1738−1740. (b) Xiang, X.-D. Combinatorial Materials Synthesis and Screening: An Integrated Materials Chip Approach to Discovery and Optimization of Functional Materials. *Annu. Rev. Mater. Sci.* **1999**, *29*, 149−171.

(12) Koinuma, H.; Takeuchi, I. Combinatorial solid-state chemistry of inorganic materials. *Nat. Mater.* **2004**, *3*, 429−438.

(13) Nakayama, A.; Suzuki, E.; Ohmori, T. Development of high throughput evaluation for photocatalyst thin-film. *Appl. Surf. Sci.* **2002**, *189*, 260−264.

(14) Mardare, A. I.; Ludwig, A.; Savan, A.; Wieck, A. D.; Hassel, A. W. Combinatorial investigation of Hf-Ta thin films and their anodic oxides. *Electrochim. Acta* **2010**, *55*, 7884−7891.

(15) Kollender, J. P.; Mardare, A. I.; Hassel, A. W. Localized Photoelectrochemistry on a Tungsten Oxide−Iron Oxide Thin Film Material Library. *ACS Comb. Sci.* **2013**, *15*, 601−608.

(16) Schäfer, D.; Mardare, C. C.; Savan, A.; Sanchez, M. D.; Mei, B.; Xia, W.; Muhler, M.; Ludwig, A.; Schuhmann, W. High-Throughput Characterization of Pt Supported on Thin Film Oxide Material Libraries Applied in the Oxygen Reduction Reaction. *Anal. Chem.* **2011**, *83*, 1916−1923.

(17) Taurino, A.; Catalano, M.; Rella, R.; Siciliano, P.; Wlodarski, W. Structural and optical properties of molybdenum-tungsten mixed oxide thin films deposited by the sol-gel technique. *J. Appl. Phys.* **2003**, *93*, 3816−3822.

(18) May, R. A.; Kondrachova, L.; Hahn, B. P.; Stevenson, K. J. Optical Constants of Electrodeposited Mixed Molybdenum-Tungsten Oxide Films Determined by Variable-Angle Spectroscopic Ellipsometry. *J. Phys. Chem. C* **2007**, *111*, 18251−18257.

(19) Gesheva, K. A.; Ivanova, T.; Marsen, B.; Cole, B.; Miller, E. L.; Hamelmann, F. Structural and surface analysis of Mo-W oxide films prepared by atmospheric pressure chemical vapor deposition. *Surf. Coat. Technol.* **2007**, *201*, 9378−9384.

(20) Khawaja, E. E.; Durrani, S. M. A.; Daous, M. A. Optical properties of thin films of WO_3, MoO_3 and mixed oxides WO_3/MoO_3. *J. Phys.: Condens. Matter* **1997**, *9*, 9381−9392.

(21) Morandi, S.; Ghiotti, G.; Chiorino, A.; Bonelli, B.; Comini, E.; Sberveglieri, G. MoO_3-WO_3 mixed oxide powder and thin films for gas sensing devices: A spectroscopic characterisation. *Sens. Actuators, B* **2005**, *111−112*, 28−35.

(22) Patil, P. R.; Patil, P. S. Preparation of mixed oxide MoO_3-WO_3 thin films by spray pyrolysis technique and their characterisation. *Thin Solid Films* **2001**, *382*, 13−22.

(23) Farveez Ahmed, H. M.; Begum, N. S. Synthesis and characterization of MoO_3-WO_3 composite thin films by liquid phase deposition technique: Investigation of its photochromic properties. *Bull. Mater. Sci.* **2013**, *36*, 45−49.

(24) Golitsyna, Y.; Hild, S., personal communication, 2014.

(25) Hafner, M.; Mardare, A. I.; Hassel, A. W. Vapour phase co-deposition of Al-Cu thin film alloys. *Phys. Status Solidi A* **2013**, *210*, 1006−1012.

(26) (a) Ohring, M. *Materials science of thin films. Deposition and structure*; Academic Press: San Diego, CA, 2002; pp 106−113. (b) Klemm, S. O.; Martin, A. G.; Lengsfeld, J.; Schauer, J.-C.; Schuhmacher, B.; Hassel, A. W. Theoretical simulation and preparation of binary and ternary combinatorial libraries by thermal PVD. *Phys. Status Solidi A* **2010**, *207*, 801−806.

(27) Ohring, M. *Materials science of thin films. Deposition and structure*; Academic Press: San Diego, CA, 2002; pp 196−198.

(28) Gesheva, K.; Szekeres, A.; Ivanova, T. Optical properties of chemical vapor deposited thin films of molybdenum and tungsten based metal oxides. *Sol. Energy Mater. Sol. Cells* **2003**, *76*, 563−576.

(29) Magnéli, A. The Crystal Structures of Mo_9O_{26} (β'-Molybdenum Oxide) and Mo_8O_{23} (β-Molybdenum Oxide). *Acta Chem. Scand.* **1948**, *2*, 501−517.

(30) (a) Gesheva, K.; Cziraki, A.; Ivanova, T.; Szekeres, A. Structure and composition of thermally annealed Mo- and W-based CVD metal oxide thin films. *Thin Solid Films* **2005**, *492*, 322−326. (b) Ivanova, T.; Gesheva, K. A.; Popkirov, G.; Ganchev, M.; Tzvetkova, E. Electrochromic properties of atmospheric CVD MoO_3 and MoO_3-WO_3 films and their application in electrochromic devices. *Mater. Sci. Eng., B* **2005**, *119*, 232−239.

(31) Ferroni, M.; Guidi, V.; Comini, E.; Sberveglieri, G.; Vomiero, A.; Della Mea, G.; Martinelli, G. Selective sublimation processing of a molybdenum-tungsten mixed oxide thin film. *J. Vac. Sci. Technol. B* **2003**, *21*, 1442−1448.

(32) Vargas-Reus, M. A.; Memarzadeh, K.; Huang, J.; Ren, G. G.; Allaker, R. P. Antimicrobial activity of nanoparticulate metal oxides against peri-implantitis pathogens. *Int. J. Antimicrob. Agents* **2012**, *40*, 135−139.

(33) Gondal, M. A.; Dastageer, M. A.; Khalil, A. Synthesis of nano-WO_3 and its catalytic activity for enhanced antimicrobial process for

water purification using laser induced photo-catalysis. *Catal. Commun.* **2009**, *11*, 214−219.
(34) Srisitthiratkul, C.; Yaipimai, W.; Intasanta, V. Environmental remediation and interfacial properties of nanosilver-decorated WO_3 nanofibers under visible light source. *IEEE 12th International Conference on Nanotechnology (IEEE-NANO)*, Birmingham, AL, Aug 20−23, 2012; pp 1−5; DOI: 10.1109/NANO.2012.6322097.
(35) Gondal, M. A.; Bagabas, A.; Dastageer, A.; Khalil, A. Synthesis, characterization, and antimicrobial application of nano-palladium-doped nano-WO_3. *J. Mol. Catal. A: Chem.* **2010**, *323*, 78−83.
(36) Gao, X.; Xiao, F.; Yang, C.; Wang, J.; Su, X. Hydrothermal fabrication of $W_{18}O_{49}$ nanowire networks with superior performance for water treatment. *J. Mater. Chem. A* **2013**, *1*, 5831−5834.
(37) Kojin, F.; Mori, M.; Noda, Y.; Inagaki, M. Preparation of carbon-coated $W_{18}O_{49}$ and its photoactivity under visible light. *Appl. Catal., B* **2008**, *78*, 202−209.